A High Order WENO Scheme for a Hierarchical Size-Structured Model

Jun Shen[1], Chi-Wang Shu[2] and Mengping Zhang[3]

Abstract

In this paper we develop a high order explicit finite difference weighted essentially non-oscillatory (WENO) scheme for solving a hierarchical size-structured population model with nonlinear growth, mortality and reproduction rates. The main technical complication is the existence of global terms in the coefficient and boundary condition for this model. We carefully design approximations to these global terms and boundary conditions to ensure high order accuracy. Comparing with the first order monotone and second order total variation bounded schemes for the same model, the high order WENO scheme is more efficient and can produce accurate results with far fewer grid points. Numerical examples including one in computational biology for the evolution of the population of *Gambussia affinis*, are presented to illustrate the good performance of the high order WENO scheme.

Key Words: hierarchical size-structured population model, WENO scheme, high order accuracy

AMS(MOS) subject classification: 65M06, 92-08

[1]Department of Mathematics, University of Science and Technology of China, Hefei, Anhui 230026, P.R. China. E-mail: jshen3@mail.ustc.edu.cn

[2]Division of Applied Mathematics, Brown University, Providence, RI 02912, USA. E-mail: shu@dam.brown.edu. Research supported in part by NSFC grant 10671190 while he was visiting the Department of Mathematics, University of Science and Technology of China, Hefei, Anhui 230026, P.R. China. Additional support was provided by ARO grant W911NF-04-1-0291 and NSF grant DMS-0510345.

[3]Department of Mathematics, University of Science and Technology of China, Hefei, Anhui 230026, P.R. China. E-mail: mpzhang@ustc.edu.cn. Research supported in part by NSFC grant 10671190.

Report Documentation Page

Form Approved
OMB No. 0704-0188

1. REPORT DATE	2. REPORT TYPE	3. DATES COVERED
2007		**00-00-2007 to 00-00-2007**

4. TITLE AND SUBTITLE	5a. CONTRACT NUMBER
A High Order WENO Scheme for a Hierarchical Size-Structured Model	5b. GRANT NUMBER
	5c. PROGRAM ELEMENT NUMBER
6. AUTHOR(S)	5d. PROJECT NUMBER
	5e. TASK NUMBER
	5f. WORK UNIT NUMBER
7. PERFORMING ORGANIZATION NAME(S) AND ADDRESS(ES) **Brown University,Division of Applied Mathematics,Providence,RI,02912**	8. PERFORMING ORGANIZATION REPORT NUMBER
9. SPONSORING/MONITORING AGENCY NAME(S) AND ADDRESS(ES)	10. SPONSOR/MONITOR'S ACRONYM(S)
	11. SPONSOR/MONITOR'S REPORT NUMBER(S)

12. DISTRIBUTION/AVAILABILITY STATEMENT
Approved for public release; distribution unlimited

13. SUPPLEMENTARY NOTES
The original document contains color images.

14. ABSTRACT

15. SUBJECT TERMS

16. SECURITY CLASSIFICATION OF:			17. LIMITATION OF ABSTRACT	18. NUMBER OF PAGES	19a. NAME OF RESPONSIBLE PERSON
a. REPORT **unclassified**	b. ABSTRACT **unclassified**	c. THIS PAGE **unclassified**		**17**	

1 Introduction

In this paper we develop a high order finite difference weighted essentially non-oscillatory (WENO) scheme for a hierarchical size-structured population model given by the following equations

$$\begin{aligned} &u_t + \left(g(x, Q(x,t))\, u\right)_x + m(x, Q(x,t))\, u = 0, \qquad (x,t) \in (0, L] \times (0, T] \\ &g(0, Q(0,t))u(0,t) = C(t) + \int_0^L \beta(x, Q(x,t))\, u(x,t)dx, \qquad t \in (0, T] \\ &u(x,0) = u^0(x), \qquad x \in [0, L] \end{aligned} \tag{1.1}$$

where $u(x,t)$ is the density of individuals having size x at time t, and the non-local term $Q(x,t)$ is defined by

$$Q(x,t) = \alpha \int_0^x \omega(\xi)u(\xi,t)d\xi + \int_x^L \omega(\xi)u(\xi,t)d\xi, \qquad 0 \le \alpha < 1 \tag{1.2}$$

for some given function ω. $Q(x,t)$ depends on the density u in a global way and is usually referred to as the *environment*. This global dependence makes the design of a high order WENO scheme complicated. Another complication is the boundary condition at size $x = 0$, which involves the function g representing the growth rate of an individual, and a global dependency on the density $u(x,t)$ for all $x \in (0, L]$. The function m in (1.1) represents the mortality rate of an individual. The function β in the boundary condition of (1.1) represents the reproduction rate of an individual, and the function C represents the inflow rate of zero-size individual from an external source. We assume that the functions g, m and β are functions of both the size x and the environment Q, which in turn depends globally on the density u, hence the problem is highly nonlinear.

The hierarchical structured population model (1.1) describes population dynamics in which the size of an individual determines its access to resources and hence to its growth or decay. This dependency is based on the environment which is a global function of the density for all sizes. We refer to, e.g. [5] for a more detailed discussion of the background and application of the hierarchical size-structured population models. These models are used

extensively in biological applications. For example, in [2], the model is applied to study the evolution of a population of *Gambussia affinis*.

Hierarchical structured population models have been studied in the literature in, e.g. [4, 5, 6, 7, 10, 12, 19], usually with more restrictive assumptions on the functions g, β and m. For example, in [5] the model (1.1) was considered for the special situation $g = g(Q)$, $\beta = \beta(Q)$, $m = m(Q)$ and $C = 0$. In [4], the model (1.1) was studied with the functions g and β depending linearly on the size x, m independent of x, and $C = 0$. In [12], (1.1) was investigated with $\alpha = 0$. The model (1.1) with the complete generality as stated above was studied in [1] and [14]. In [1] an implicit first order finite difference scheme was analyzed and its stability and convergence, as well as the existence, uniqueness and well-posedness (in L^1 norm) of bounded variation weak solutions for (1.1) were proved. In [14] we developed and analyzed two explicit finite difference schemes, namely a first order upwind scheme and a second order high resolution scheme, for solving (1.1). Stability and convergence were proved for both schemes in [14].

Even though the second order high resolution scheme developed in [14] is significantly more accurate than first order schemes, the performance can be further improved by an even higher order scheme. Of course, since the solution of this model can be discontinuous, a nonlinearly stable high order scheme which can maintain high order accuracy in smooth regions and have sharp, monotone discontinuity transitions would be desirable. In this paper we develop an explicit finite difference WENO scheme for solving (1.1), following the successful class of WENO schemes for computational fluid dynamics and for general conservation laws [11, 15, 16, 17]. The main technical complication for this development is the existence of global terms in the coefficient and boundary condition of this model. We carefully design approximations to these global terms and boundary conditions to ensure high order accuracy. We then provide numerical examples to demonstrate the capability of the scheme in solving smooth and discontinuous solutions. For a smooth solution, we verify that the complicated global boundary condition and coefficients are all implemented

accurately and the designed high order accuracy can be achieved. The numerical examples also include one in computational biology for the evolution of the population of *Gambussia affinis*, for which our results with the fifth order accurate WENO scheme have a comparable resolution as the second order accurate scheme used in [2] with far fewer grid points.

We recall ([1] and [14]) that the following assumptions are made on the model functions:

- (H1) $g(x,Q)$ is twice continuously differentiable with respect to x and Q, $g(x,Q) > 0$ for $x \in [0,L)$, $g(L,Q) = 0$, and $g_Q(x,Q) \leq 0$.
- (H2) $m(x,Q)$ is nonnegative continuously differentiable with respect to x and Q.
- (H3) $\beta(x,Q)$ is nonnegative continuously differentiable with respect to x and Q. Furthermore, there is a constant $\omega_1 > 0$ such that $\sup_{(x,Q)\in[0,L]\times[0,\infty)} \beta(x,Q) \leq \omega_1$.
- (H4) $\omega(x)$ is nonnegative continuously differentiable.
- (H5) $C(t)$ is nonnegative continuously differentiable.
- (H6) $u^0 \in BV[0,L]$ and $u^0(x) \geq 0$.

In section 2, we present the detailed construction of an explicit, fifth order accurate finite difference WENO scheme for solving (1.1). Section 3 contains numerical examples demonstrating the capability of this WENO scheme. Concluding remarks are given in section 4.

2 A fifth order accurate finite difference WENO scheme

First we briefly describe the notations that we will use. We assume the spatial domain $[0,L]$ is divided into N cells with cell boundary points denoted by x_j, for $0 \leq j \leq N$, $x_0 = 0$ and $x_N = L$. For simplicity of presentation we will assume that the mesh is uniform of size Δx, namely $x_j = j\Delta x$. Our scheme can also be designed on a smoothly varying non-uniform mesh. We denote the time step by Δt. In fact, this time step $\Delta t = \Delta t^n = t^{n+1} - t^n$ could

change from one step to the next, based on stability conditions, but we use the same notation Δt without the superscript n since we will only consider one-step time discretization (Runge-Kutta). We shall denote by u_j^n and Q_j^n the finite difference approximations of $u(x_j, t^n)$ and $Q(x_j, t^n)$, respectively. We also denote

$$g_j^n = g(x_j, Q_j^n), \;\; \beta_j^n = \beta(x_j, Q_j^n), \;\; m_j^n = m(x_j, Q_j^n), \;\; \omega_j = \omega(x_j), \;\; C^n = C(t^n)$$

and we define the standard discrete L^1 and L^∞ norms of the grid function u^n by

$$\|u^n\|_1 = \sum_{j=1}^{N} |u_j^n| \Delta x, \qquad \|u^n\|_\infty = \max_{0 \le j \le N} |u_j^n|.$$

For semi-discrete approximations the superscript n referring to the time level is absent.

We now describe our development of a fifth order finite difference WENO scheme for solving (1.1), following the construction of finite difference WENO schemes in [11, 15, 16]. Notice that we choose fifth order accuracy since it is the most often used WENO scheme, however our scheme can also be designed for other orders of accuracy along the same lines, see, e.g. [3]. The semi-discrete fifth order high finite difference WENO scheme is defined by the following conservative approximation

$$\frac{d}{dt} u_j + \frac{1}{\Delta x} \left(\hat{f}_{j+1/2} - \hat{f}_{j-1/2} \right) + m_j u_j = 0, \qquad 1 \le j \le N, \tag{2.1}$$

where the fifth order accurate numerical flux $\hat{f}_{j+1/2}$ is defined by a weighted average of three third order accurate fluxes

$$\hat{f}_{j+1/2} = w_1 \hat{f}^1_{j+1/2} + w_2 \hat{f}^2_{j+1/2} + w_3 \hat{f}^3_{j+1/2}, \qquad j = 0, 1, \cdots, N.$$

The coefficients w_1, w_2 and w_3 are called the nonlinear weights.

The three third order accurate fluxes $\hat{f}^1_{j+1/2}$, $\hat{f}^2_{j+1/2}$ and $\hat{f}^3_{j+1/2}$ are obtained following the procedure in [11, 16] and are given explicitly by

$$\begin{cases} \hat{f}^1_{j+1/2} = \frac{1}{3} f_{j-2} - \frac{7}{6} f_{j-1} + \frac{11}{6} f_j \\ \hat{f}^2_{j+1/2} = -\frac{1}{6} f_{j-1} + \frac{5}{6} f_j + \frac{1}{3} f_{j+1} \qquad j = 2, \cdots, N-2, \\ \hat{f}^3_{j+1/2} = \frac{1}{3} f_j + \frac{5}{6} f_{j+1} - \frac{1}{6} f_{j+2} \end{cases}$$

in the middle of the computational domain. For the two points from the left boundary, these fluxes are given by

$$\begin{cases} \hat{f}^1_{1/2} = \frac{1}{3}f_0 + \frac{5}{6}f_1 - \frac{1}{6}f_2 \\ \hat{f}^2_{1/2} = \frac{11}{6}f_1 - \frac{7}{6}f_2 + \frac{1}{3}f_3 \\ \hat{f}^3_{1/2} = \frac{13}{3}f_2 - \frac{31}{6}f_3 + \frac{11}{6}f_4, \end{cases} \qquad \begin{cases} \hat{f}^1_{3/2} = -\frac{1}{6}f_0 + \frac{5}{6}f_1 + \frac{1}{3}f_2 \\ \hat{f}^2_{3/2} = \frac{1}{3}f_1 + \frac{5}{6}f_2 - \frac{1}{6}f_3 \\ \hat{f}^3_{3/2} = \frac{11}{6}f_2 - \frac{7}{6}f_3 + \frac{1}{3}f_4. \end{cases}$$

Similarly, for the two points from the right boundary, they are given by

$$\begin{cases} \hat{f}^1_{N-1/2} = \frac{11}{6}f_{N-4} - \frac{31}{6}f_{N-3} + \frac{13}{3}f_{N-2} \\ \hat{f}^2_{N-1/2} = \frac{1}{3}f_{N-3} - \frac{7}{6}f_{N-2} + \frac{11}{6}f_{N-1} \\ \hat{f}^3_{N-1/2} = -\frac{1}{6}f_{N-2} + \frac{5}{6}f_{N-1} + \frac{1}{3}f_N, \end{cases} \qquad \begin{cases} \hat{f}^1_{N+1/2} = \frac{13}{3}f_{N-4} - \frac{67}{6}f_{N-3} + \frac{47}{6}f_{N-2} \\ \hat{f}^2_{N+1/2} = \frac{11}{6}f_{N-3} - \frac{31}{6}f_{N-2} + \frac{13}{3}f_{N-1} \\ \hat{f}^3_{N+1/2} = \frac{1}{3}f_{N-2} - \frac{7}{6}f_{N-1} + \frac{11}{6}f_N. \end{cases}$$

In all the formulas above, $f_j = g_j u_j$ are the point values of the flux function $g(x, Q(x,t))\, u$.

The nonlinear weights are defined by

$$w_r = \frac{\alpha_r}{\sum_{s=1}^3 \alpha_s}, \qquad \alpha_r = \frac{d_r}{(\varepsilon + \beta_r)^2}, \qquad r = 1, 2, 3. \tag{2.2}$$

Here d_r are the linear weights which can guarantee fifth order accuracy, and ε is a small positive number introduced to avoid the denominator to become 0 and is usually taken as $\varepsilon = 10^{-6}$ in numerical tests. β_r are the so-called "smoothness indicators", which measure the smoothness of the function in the relevant stencils. We adopt the smoothness indicators introduced in [11]

$$\beta_r = \sum_{\ell=1}^{2} \Delta x^{2\ell-1} \int_{x_{j-1/2}}^{x_{j+1/2}} \left(\frac{d^\ell}{dx^\ell} p_r(x) \right)^2 dx$$

where $p_r(x)$ is the relevant quadratic reconstruction polynomial to yield the flux $\hat{f}^r_{j+1/2}$. Notice that, since the coefficient $g(x, Q(x,t))$ is positive, upwinding is biasing the stencil to the left, and the measurement of smoothness is for the interval $[x_{j-1/2}, x_{j+1/2}]$ which is to the left of the flux location $x_{j+1/2}$. We can work out the explicit formulas for these smoothness indicators. These explicit formulas, together with the linear weights d_r, are listed below. For the points inside the computational domain, with $1 \le j \le N-2$, we have

$$\begin{cases} \beta_1 = \frac{13}{12}(f_{j-2} - f_{j-1} + f_j)^2 + \frac{1}{4}(f_{j-2} - 4f_{j-1} + 3f_j)^2 \\ \beta_2 = \frac{13}{12}(f_{j-1} - 2f_j + f_{j+1})^2 + \frac{1}{4}(f_{j-1} - f_{j+1})^2 \\ \beta_3 = \frac{13}{12}(f_j - 2f_{j+1} + f_{j+2})^2 + \frac{1}{4}(3f_j - 4f_{j+1} + f_{j+2})^2 \end{cases}$$

and

$$d_1 = 1/10, \qquad d_2 = 3/5, \qquad d_3 = 3/10.$$

For $j = N-1$, we have

$$\begin{cases} \beta_1 = \frac{10}{3} f_{N-4}^2 + \frac{61}{3} f_{N-3}^2 + \frac{22}{3} f_{N-2}^2 - \frac{49}{3} f_{N-4} f_{N-3} + \frac{29}{3} f_{N-4} f_{N-2} - \frac{73}{3} f_{N-3} f_{N-2} \\ \beta_2 = \frac{4}{3} f_{N-3}^2 + \frac{25}{3} f_{N-2}^2 + \frac{10}{3} f_{N-1}^2 - \frac{19}{3} f_{N-3} f_{N-2} + \frac{11}{3} f_{N-3} f_{N-1} - \frac{31}{3} f_{N-2} f_{N-1} \\ \beta_3 = \frac{4}{3} f_{N-2}^2 + \frac{13}{3} f_{N-1}^2 + \frac{4}{3} f_N^2 - \frac{13}{3} f_{N-2} f_{N-1} + \frac{5}{3} f_{N-2} f_N - \frac{13}{3} f_{N-1} f_N \end{cases}$$

and

$$d_1 = -3/110, \qquad d_2 = 47/110, \qquad d_3 = 3/5.$$

For $j = N$, we have

$$\begin{cases} \beta_1 = \frac{22}{3} f_{N-4}^2 + \frac{121}{3} f_{N-3}^2 + \frac{40}{3} f_{N-2}^2 - \frac{103}{3} f_{N-4} f_{N-3} + \frac{59}{3} f_{N-4} f_{N-2} - \frac{139}{3} f_{N-3} f_{N-2} \\ \beta_2 = \frac{10}{3} f_{N-3}^2 + \frac{61}{3} f_{N-2}^2 + \frac{22}{3} f_{N-1}^2 - \frac{49}{3} f_{N-3} u_{N-2} + \frac{29}{3} f_{N-3} f_{N-1} - \frac{73}{3} f_{N-2} f_{N-1} \\ \beta_3 = \frac{4}{3} f_{N-2}^2 + \frac{25}{3} f_{N-1}^2 + \frac{10}{3} f_N^2 - \frac{19}{3} f_{N-2} u_{N-1} + \frac{11}{3} f_{N-2} f_N - \frac{31}{3} f_{N-1} f_N \end{cases}$$

and

$$d_1 = 3/65, \qquad d_2 = -417/1430 \qquad d_3 = 137/110.$$

Notice that some of the linear weights for $j = N-1$ and $j = N$ are negative. We have used the technique introduced in [15] to treat these negative weights. We refer to [15] for the details and will not describe them here.

For the two points from the left boundary, we could also use the smoothness indicators and nonlinear weights as those for the right boundary, in a mirror symmetric fashion. Our computational experience however indicates that it is better to use simply the linear weights for these two points, which is the practice that we have adopted in the numerical experiments in next section.

The global boundary condition at the left is implemented by a fifth order composite rule

$$g_0 u_0 = C + \sum_{j=0}^{N}{}' \, \beta_j u_j \Delta x, \tag{2.3}$$

where the special summation notation is defined by

$$\begin{aligned} \sum_{j=j_1}^{j_2}{}' \, a_j \;\; = \;\; & \frac{251}{720} a_{j_1} + \frac{299}{240} a_{j_1+1} + \frac{211}{240} a_{j_1+2} + \frac{739}{720} a_{j_1+3} + \\ & \frac{739}{720} a_{j_2-3} + \frac{211}{240} a_{j_2-2} + \frac{299}{240} a_{j_2-1} + \frac{251}{720} a_{j_2} + \sum_{j=j_1+4}^{j_2-4} a_j \end{aligned}$$

if $j_2 - j_1 \geq 7$. The environment is computed also by the same fifth order composite rule, except for the integrals with $j_2 - j_1 \leq 6$ and the integral over the first interval which is computed avoiding the usage of u_0. Letting $A = (\frac{55}{24}\omega_1 u_1 - \frac{59}{24}\omega_2 u_2 + \frac{37}{24}\omega_3 u_3 - \frac{9}{24}\omega_4 u_4)\Delta x$ be the fifth accurate approximation to $\int_{x_0}^{x_1} \omega(x)u(x,t)\,dx$, we have

$$
\begin{aligned}
Q_j &= A + \alpha \sum_{i=1}^{j}{}' \, \omega_i u_i \Delta x + \sum_{i=j}^{N}{}' \, \omega_i u_i \Delta x, \qquad 8 \leq j \leq N-7, \\
Q_0 &= A + \sum_{i=1}^{N}{}' \, \omega_i u_i \Delta x, \qquad Q_1 = \alpha A + \sum_{i=1}^{N}{}' \, \omega_i u_i \Delta x, \qquad Q_N = \alpha Q_0, \\
Q_2 &= \alpha \Delta x \left(\frac{8}{3}\omega_1 u_1 - \frac{5}{3}\omega_2 u_2 + \frac{4}{3}\omega_3 u_3 - \frac{1}{3}\omega_4 u_4 \right) + \sum_{i=2}^{N}{}' \, \omega_i u_i \Delta x, \\
Q_3 &= \alpha \Delta x \left(\frac{21}{8}\omega_1 u_1 - \frac{9}{8}\omega_2 u_2 + \frac{15}{8}\omega_3 u_3 - \frac{3}{8}\omega_4 u_4 \right) + \sum_{i=3}^{N}{}' \, \omega_i u_i \Delta x, \\
Q_4 &= \alpha \Delta x \left(\frac{21}{8}\omega_1 u_1 - \frac{7}{6}\omega_2 u_2 + \frac{29}{12}\omega_3 u_3 + \frac{1}{6}\omega_4 u_4 - \frac{1}{24}\omega_5 u_5 \right) + \sum_{i=4}^{N}{}' \, \omega_i u_i^n \Delta x, \\
Q_5 &= \alpha \Delta x \left(\frac{21}{8}\omega_1 u_1 - \frac{7}{6}\omega_2 u_2 + \frac{19}{8}\omega_3 u_3 + \frac{17}{24}\omega_4 u_4 + \frac{1}{2}\omega_5 u_5 - \frac{1}{24}\omega_6 u_6 \right) + \sum_{i=5}^{N}{}' \, \omega_i u_i \Delta x, \\
Q_6 &= \alpha \Delta x \left(\frac{21}{8}\omega_1 u_1 - \frac{7}{6}\omega_2 u_2 + \frac{19}{8}\omega_3 u_3 + \frac{2}{3}\omega_4 u_4 + \frac{25}{24}\omega_5 u_5 + \frac{1}{2}\omega_6 u_6 - \frac{1}{24}\omega_7 u_7 \right) \\
&\quad + \sum_{i=6}^{N}{}' \, \omega_i u_i \Delta x, \\
Q_7 &= \alpha \Delta x \left(\frac{21}{8}\omega_1 u_1 - \frac{7}{6}\omega_2 u_2 + \frac{19}{8}\omega_3 u_3 + \frac{2}{3}\omega_4 u_4 + \omega_5 u_5 + \frac{25}{24}\omega_6 u_6 + \frac{1}{2}\omega_7 u_7 - \frac{1}{24}\omega_8 u_8 \right) \\
&\quad + \sum_{i=7}^{N}{}' \, \omega_i u_i \Delta x, \\
Q_{N-1} &= \Delta x \left(\frac{9}{24}\omega_N u_N + \frac{19}{24}\omega_{N-1} u_{N-1} - \frac{5}{24}\omega_{N-2} u_{N-2} + \frac{1}{24}\omega_{N-3} u_{N-3} \right) \\
&\quad + \alpha \left(A + \sum_{i=1}^{N-1}{}' \, \omega_i u_i \Delta x \right), \\
Q_{N-2} &= \Delta x \left(\frac{1}{3}\omega_N u_N + \frac{4}{3}\omega_{N-1} u_{N-1} + \frac{1}{3}\omega_{N-2} u_{N-2} \right) + \alpha \left(A + \sum_{i=1}^{N-2}{}' \, \omega_i u_i \Delta x \right), \\
Q_{N-3} &= \Delta x \left(\frac{1}{3}\omega_N u_N + \frac{31}{24}\omega_{N-1} u_{N-1} + \frac{7}{8}\omega_{N-2} u_{N-2} + \frac{13}{24}\omega_{N-3} u_{N-3} - \frac{1}{24}\omega_{N-4} u_{N-4} \right)
\end{aligned}
$$

$$
\begin{aligned}
&+\alpha\left(A+\sum_{i=1}^{N-3}{}'\,\omega_i u_i\Delta x\right),\\
Q_{N-4} &= \Delta x\left(\frac{1}{3}\omega_N u_N+\frac{31}{24}\omega_{N-1}u_{N-1}+\frac{5}{6}\omega_{N-2}u_{N-2}+\frac{13}{12}\omega_{N-3}u_{N-3}+\frac{1}{2}\omega_{N-4}u_{N-4}\right.\\
&\left.-\frac{1}{24}\omega_{N-5}u_{N-5}\right)+\alpha\left(A+\sum_{i=1}^{N-4}{}'\,\omega_i u_i\Delta x\right),\\
Q_{N-5} &= \Delta x\left(\frac{1}{3}\omega_N u_N+\frac{31}{24}\omega_{N-1}u_{N-1}+\frac{5}{6}\omega_{N-2}u_{N-2}+\frac{25}{24}\omega_{N-3}u_{N-3}+\frac{25}{24}\omega_{N-4}u_{N-4}\right.\\
&\left.+\frac{1}{2}\omega_{N-5}u_{N-5}-\frac{1}{24}\omega_{N-6}u_{N-6}\right)+\alpha\left(A+\sum_{i=1}^{N-5}{}'\,\omega_i u_i\Delta x\right),\\
Q_{N-6} &= \Delta x\left(\frac{1}{3}\omega_N u_N+\frac{31}{24}\omega_{N-1}u_{N-1}+\frac{5}{6}\omega_{N-2}u_{N-2}+\frac{25}{24}\omega_{N-3}u_{N-3}+\omega_{N-4}u_{N-4}\right.\\
&\left.+\frac{25}{24}\omega_{N-5}u_{N-5}+\frac{1}{2}\omega_{N-6}u_{N-6}-\frac{1}{24}\omega_{N-7}u_{N-7}\right)+\alpha\left(A+\sum_{i=1}^{N-6}{}'\,\omega_i u_i\Delta x\right).
\end{aligned}
$$

Notice that these approximations to Q_j are all fifth order accurate. The initial condition is taken as

$$u_j^0 = u^0(x_j), \qquad j = 1, 2, \cdots, N.$$

Using the notation $\lambda = \frac{\Delta t}{\Delta x}$, we can write the Euler forward time discretization of the semi-discrete scheme (2.1) as

$$u_j^{n+1} = u_j^n - \lambda(\hat{f}_{j+1/2}^n - \hat{f}_{j-1/2}^n) - \Delta t m_j^n u_j^n, \qquad j = 1, 2, \cdots, N. \tag{2.4}$$

This, together with the boundary condition (2.3) for u_0^n, provides a complete description of the explicit time marching fifth order finite difference WENO scheme. In order to obtain higher order accuracy in time without compromising the nonlinear stability of the WENO scheme, we use the total variation diminishing (TVD) high order Runge-Kutta time discretization in [18], see also [8, 9]. If we denote the ordinary differential equation system (2.1) by

$$\frac{d}{dt}u_j - L(u,t)_j = 0,$$

then the third order TVD Runge-Kutta method in [18] that we use in next section is given

by

$$\begin{aligned} u^{(1)} &= u^n + \Delta t L(u^n, t^n) \\ u^{(2)} &= \frac{3}{4}u^n + \frac{1}{4}\left(u^{(1)} + \Delta t L(u^{(1)}, t^n + \Delta t)\right) \\ u^{n+1} &= \frac{1}{3}u^n + \frac{2}{3}\left(u^{(2)} + \Delta t L\left(u^{(2)}, t^n + \frac{1}{2}\Delta t\right)\right). \end{aligned} \tag{2.5}$$

Clearly, this is just three Euler forward time discretizations with suitable coefficients, hence its implementation does not introduce any difficulty.

3 Numerical examples

In this section we perform numerical experiments to demonstrate the performance of the fifth order WENO scheme developed in the previous section. We use the third order TVD Runge-Kutta time discretization (2.5) with a CFL condition

$$\Delta t^n = 0.6\Delta x / \|g(x, Q^n) + m(x, Q^n)\Delta x\|_\infty$$

unless otherwise stated.

In our first example, we use the initial condition $u^0(x) = -x^2 + x + 1$, and take the parameters and functions in (1.1) and (1.2) as $L = 1$, $\alpha = 0.5$, $\omega(x) = 1$, $g(x, Q) = (1 - x)(5 - x + x^2/2 - Q)$, $m(x, Q) = 4 + 2Q + (1 - x)^2/2$, and $\beta(x, Q) = (1 + x)(2 - Q)$. The purpose of this example is to show that the WENO scheme is non-oscillatory in the presence of solution discontinuities. For this purpose we take $C(t) = 3$, which causes an incompatibility of the boundary data and the initial condition at the origin and generates a discontinuity in the solution which moves from the left boundary into the computational domain. The numerical solutions using $N = 100$ uniformly spaced grid points for the first order monotone scheme [14], the second order high resolution scheme [14], and the fifth order WENO scheme are plotted in Fig. 3.1. We can see clearly that our fifth order WENO scheme can resolve the discontinuity sharper than the first order monotone scheme and the second order high resolution scheme, without introducing spurious numerical oscillations.

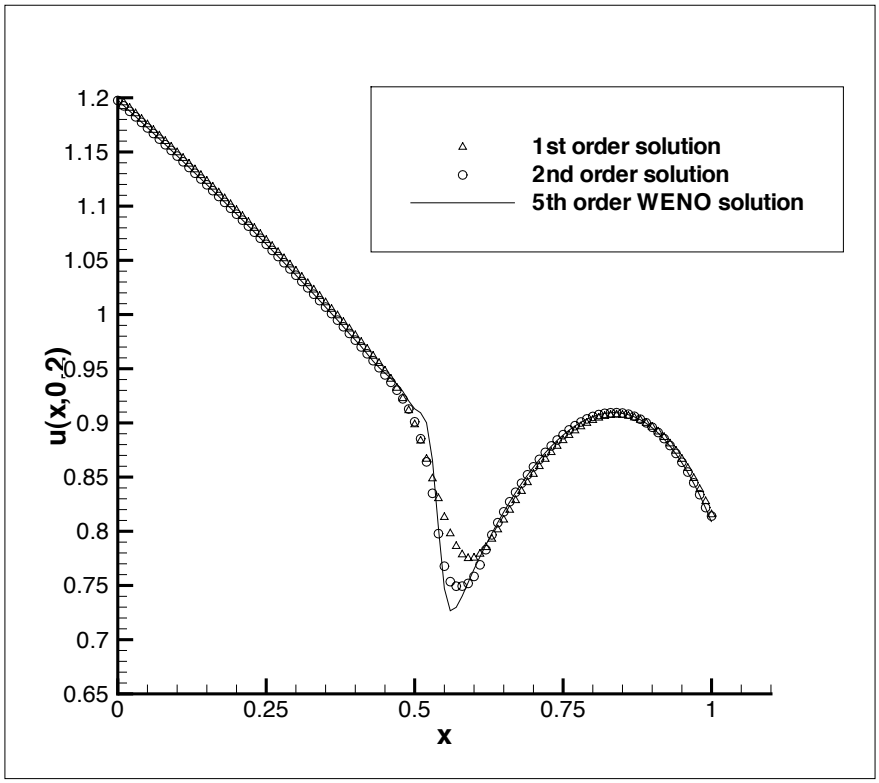

Figure 3.1: Numerical solutions with $N = 100$ uniform grid points, using the first order monotone scheme in [14] (triangles), the second order high resolution scheme in [14] (circles), and the fifth order WENO scheme (solid line).

The second example is chosen to demonstrate that our fifth order WENO scheme can achieve its designed accuracy for smooth solutions. For this purpose we take $g(x, Q) = -2e^{x-1} + 2$, $\beta(x, Q) = 2$, $m(x, Q) = 1$, $L = 1$, $\omega(x) = 1$, $\alpha = 0.5$, the initial condition $u^0(x) = e^{-x}$, and $C(t) = 0$. For these choices the equation (1.1) has a smooth exact solution $u(x, t) = e^{t-x}$. The L^∞ and L^1 errors and orders of accuracy of our fifth order WENO scheme are listed in Table 3.1. We can see that the designed order of accuracy is obtained for this smooth solution in the L^1 norm. The order in the L^∞ norm is reduced by one order because near the boundary, the cancellation of the neighboring numerical fluxes to generate an extra order of accuracy is no longer valid. For this test case we further reduce the time step to ensure that the spatial error dominates in the solution.

Our third example is from computational biology [2], for the simulation of the population

Table 3.1: L^∞ and L^1 errors and numerical orders of accuracy of the fifth order WENO scheme using N uniformly spaced mesh points.

N	L^∞ error	order	L^1 error	order
10	0.21E-03		0.25E-04	
20	0.95E-05	4.46	0.64E-06	5.28
40	0.52E-06	4.20	0.19E-07	5.07
80	0.30E-07	4.10	0.59E-09	5.03
160	0.18E-08	4.08	0.18E-10	5.02
320	0.10E-09	4.12	0.49E-12	5.20

evolution of *Gambussia affinis*. This model is given by the equation (1.1), written in a slightly different form as

$$\begin{aligned} &u_t + \left(g(x,t)\,u\right)_x + m(x,Q(t),t)\,u = 0, \qquad (x,t) \in [9,63]\times(0,T] \\ &g(9,t)u(9,t) = \int_9^{63} \beta(x,t)\,u(x,t)dx, \qquad t \in (0,T] \\ &u(x,0) = u^0(x), \qquad x \in [9,63] \end{aligned} \tag{3.1}$$

The non-local term $Q(t)$ is defined by

$$Q(t) = \int_9^{63} \omega(x)u(x,t)dx \tag{3.2}$$

The initial condition and the functions in (3.1) and (3.2) are defined as in [2]. In particular,

$$\beta(x,t) = \beta(x)T_\beta(t), \quad g(x,t) = g(x)T_g(t), \quad m(x,Q(t),t) = m(x,Q(t))T_m(t),$$

where $\beta(x)$ is a smooth spline function to fit the data in Krumholtz [13] by using a MATLAB function called *csaps* (see Fig. 1 in [2]), $T_\beta(t)$ is defined by

$$T_\beta(t) = \begin{cases} (\frac{t}{30})^3(1 - \frac{t-30}{10} + \frac{(t-30)^2}{150}), & 0 \le t \le 30 \\ 1, & 30 \le t \le 90 \\ -(\frac{t-120}{30})^3(1 + \frac{t-90}{10} + \frac{(t-90)^2}{150}), & 90 \le t \le 120 \\ 0, & 120 \le t \le 365 \end{cases}$$

and it is periodically extended thereafter

$$T_\beta(t + 365n) = T_\beta(t), \qquad n = 1, 2, \cdots .$$

The function $g(x)$ is defined as

$$g(x) = \frac{63}{80.2}\left(1 - \frac{x}{63}\right), \quad 9 \le x \le 63$$

and the function $T_g(t)$ is defined as

$$T_g(t) = 0.2 + 0.8T_\beta(t).$$

The function $m(x, Q)$ is given by

$$m(x,Q) = \begin{cases} 0.1\exp(-C/Q), & 9 \le x \le 31 \\ 0.1\exp(-C/Q) - (0.023 - 0.1\exp(-C/Q)) & \\ \quad \times (x-31)^3(1-3(x-32)(65-2x)), & 31 \le x \le 32 \\ 0.023, & 32 \le x \le 63 \end{cases} \tag{3.3}$$

where the constant C will be prescribed later. The function $T_m(t)$ is given by

$$T_m(t) = 2 - T_\beta(t),$$

and finally the function $\omega(x)$ is given by

$$\omega(x) = \begin{cases} 2, & 9 \le x \le 30 \\ -2(x-31)^3(1+3(x-30)(2x-59)), & 30 < x < 31 \\ 0. & 31 \le x \le 63 \end{cases}$$

The initial condition is given as

$$u_0(x) = \begin{cases} 0, & 9 \le x \le 34 \\ 5(1+\frac{x-38}{4})^3, & 34 < x < 38 \\ 5 + 15(\frac{x-38}{4}) + 15(\frac{x-38}{4})^2 + 30(\frac{x-38}{4})^3(\frac{x-46}{4}), & 38 \le x \le 42 \\ 5(2-\frac{x-38}{4})^3, & 42 \le x \le 46 \\ 0. & 46 \le x \le 63 \end{cases}$$

We note that not all the assumptions (H1)-(H6) outlined in the introduction are satisfied in this example. However, our fifth order WENO scheme performs nicely and gives accurate results with far fewer grid points than the second order schemes in [2] and [14]. In Fig. 3.2, we plot the population density u at $t = 365$ using the fifth order WENO scheme with $N = 135$ uniformly spaced grid points. In this simulation the constant C in (3.3) is taken as 2000 as in [2]. For the purpose of comparison, the simulation result using the second order high resolution scheme in [14] with $N = 540$ uniformly spaced grid points is also plotted in

Fig. 3.2. We can observe that the WENO scheme gives better resolution than the second order scheme even though the latter uses fourfold as many grid points. Comparing with the second order box method using $N = 730$ grid points in [2], Fig. 4, we can see that the second order box method in [2] performs similarly as the second order high resolution scheme in [14], and the fifth order WENO scheme clearly outperforms both of them.

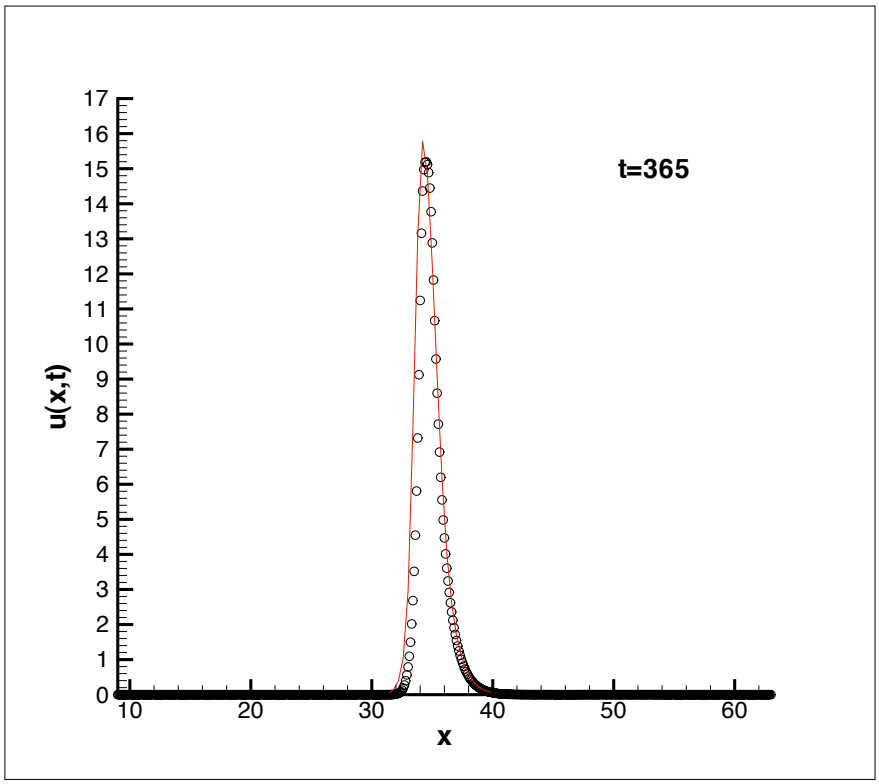

Figure 3.2: Population density u as a function of the length at $t = 365$. Solid line: solution of the fifth order WENO scheme with $N = 135$ uniformly spaced grid points; Circle symbols: solution of the second order high resolution scheme [14] with $N = 540$ uniformly spaced grid points.

In order to fully assess the resolution power of the high order WENO scheme for long time simulation with coarse meshes, we simulate this model for 10 years and plot the total population (the integral of the density u over the length) in Fig. 3.3, for two different values of C in (3.3), namely $C = 2000$ for the left picture and $C = 200000$ for the right picture, as in [2], Figures 7 and 12. For this test problem, we perform numerical tests with different number of mesh points and report the results using the coarsest meshes of different numerical

methods to obtain the visually satisfactory resolution. We are pleasantly surprised to observe that the WENO scheme with only $N = 20$ uniformly spaced grid points is enough to yield the satisfactory resolution as shown in Fig. 3.3, while the second order high resolution scheme in [14] needs $N = 108$ points to achieve comparable resolution.

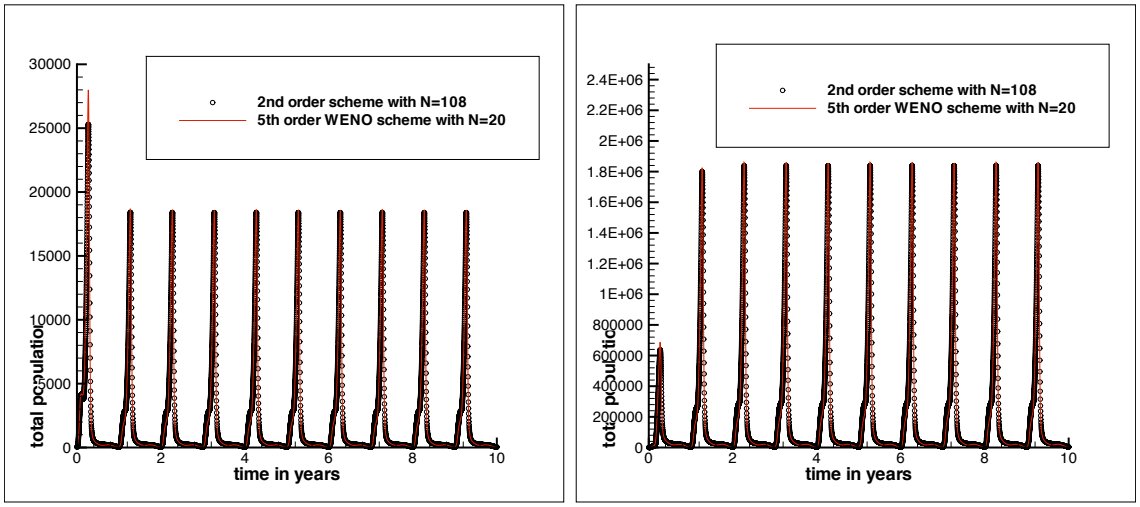

Figure 3.3: Evolution of the total population for ten years. Left: $C = 2000$; Right: $C = 200000$. Solid line: solution of the fifth order WENO scheme with $N = 20$ uniformly spaced grid points; Circle symbols: solution of the second order high resolution scheme [14] with $N = 108$ uniformly spaced grid points.

4 Concluding remarks

We have developed a fifth order explicit finite difference WENO scheme for solving a hierarchical size-structured population model with nonlinear growth, mortality and reproduction rates, which contains global terms both for the boundary condition and for the coefficients in the equations. Numerical results are provided to demonstrate the capability of this WENO scheme in resolving smooth as well as discontinuous solutions. For smooth solutions the fifth order WENO scheme achieves its designed order of accuracy. For discontinuous solutions, the WENO scheme gives sharp and non-oscillatory discontinuity transitions. An application of the scheme to a problem in computational biology for the evolution of the population of *Gambussia affinis* indicates that the WENO scheme can achieve good resolution for long

time simulation with very coarse meshes, hence it is much more efficient than lower order schemes for such simulations.

References

[1] A.S. Ackleh, K. Deng and S. Hu, *A quasilinear hierarchical size structured model: well-posedness and approximation*, Applied Mathematics and Optimization, 51 (2005), 35-59.

[2] O. Angulo, A. Durán and J.C. López-Marcos, *Numerical study of size-structured population models: A case of Gambussia affinis*, Comptes Rendus Biologies, 328 (2005), 387-402.

[3] D.S. Balsara and C.-W. Shu, *Monotonicity preserving weighted essentially non-oscillatory schemes with increasingly high order of accuracy*, Journal of Computational Physics, 160 (2000), 405-452.

[4] K.W. Blayneh, *Hierarchical size-structured population model*, Dynamical Systems and Applications, 9 (2002), 527-540.

[5] A. Calsina and J. Saldana, *Asymptotic behavior of a model of hierarchically structured population dynamics*, Journal of Mathematical Biology, 35 (1997), 967-987.

[6] J.M. Cushing, *The dynamics of hierarchical age-structured population*, Journal of Mathematical Biology, 32 (1994), 705-729.

[7] J.M. Cushing and J. Li, *Juvenile versus adult competition*, Journal of Mathematical Biology, 29 (1991), 457-473.

[8] S. Gottlieb and C.-W. Shu, *Total variation diminishing Runge-Kutta schemes*, Mathematics of Computation, 67 (1998), 73-85.

[9] S. Gottlieb, C.-W. Shu and E. Tadmor, *Strong stability preserving high order time discretization methods*, SIAM Review, 43 (2001), 89-112.

[10] S.M. Henson and J.M. Cushing, *Hierarchical models of intra-specific competition: scramble versus contest*, Journal of Mathematical Biology, 34 (1996), 755-772.

[11] G. Jiang and C.-W. Shu, *Efficient implementation of weighted ENO schemes*, Journal of Computational Physics, 126 (1996), 202-228.

[12] E.A. Kraev, *Existence and uniqueness for height structured hierarchical population models*, Natural Resource Modeling, 14 (2001), 45-70.

[13] L.A. Krumholtz, *Reproduction in the western mosquitofish, Gambusia affinis (Baird and Girard), and its use in mosquito control*, Ecological Monographs, 18 (1948), 1-43.

[14] J. Shen, C.-W. Shu and M. Zhang, *High resolution schemes for a hierarchical size-structured model*, SIAM Journal on Numerical Analysis, 45 (2007), 352-370.

[15] J. Shi, C. Hu and C.-W. Shu, *A technique of treating negative weights in WENO schemes*, Journal of Computational Physics, 175 (2002), 108-127.

[16] C.-W. Shu, *Essentially non-oscillatory and weighted essentially non-oscillatory schemes for hyperbolic conservation laws*, in *Advanced Numerical Approximation of Nonlinear Hyperbolic Equations*, B. Cockburn, C. Johnson, C.-W. Shu and E. Tadmor (Editor: A. Quarteroni), Lecture Notes in Mathematics, volume 1697, Springer, 1998, pp.325-432.

[17] C.-W. Shu, *High-order finite difference and finite volume WENO schemes and discontinuous Galerkin methods for CFD*, International Journal of Computational Fluid Dynamics, 17 (2003), 107-118.

[18] C.-W. Shu and S. Osher, *Efficient implementation of essentially non-oscillatory shock-capturing schemes*, Journal of Computational Physics, 77 (1988), 439-471.

[19] J. Weiner and S.X. Thomas, *Size variability and competition in plant monocultures*, Oikos, 47 (1986), 211-222.